

ARTICLE

Received 5 Jun 2014 | Accepted 8 Jan 2015 | Published 18 Feb 2015

DOI: 10.1038/ncomms7243

A cnidarian homologue of an insect gustatory receptor functions in developmental body patterning

Michael Saina¹, Henriette Busengdal², Chiara Sinigaglia^{2,†}, Libero Petrone³, Paola Oliveri³, Fabian Rentzsch² & Richard Benton¹

Insect gustatory and odorant receptors (GRs and ORs) form a superfamily of novel transmembrane proteins, which are expressed in chemosensory neurons that detect environmental stimuli. Here we identify homologues of GRs (*Gustatory receptor-like (Grl)* genes) in genomes across Protostomia, Deuterostomia and non-Bilateria. Surprisingly, two *Grls* in the cnidarian *Nematostella vectensis*, *NvecGrl1* and *NvecGrl2*, are expressed early in development, in the blastula and gastrula, but not at later stages when a putative chemosensory organ forms. *NvecGrl1* transcripts are detected around the aboral pole, considered the equivalent to the head-forming region of Bilateria. Morpholino-mediated knockdown of *NvecGrl1* causes developmental patterning defects of this region, leading to animals lacking the apical sensory organ. A deuterostome *Grl* from the sea urchin *Strongylocentrotus purpuratus* displays similar patterns of developmental expression. These results reveal an early evolutionary origin of the insect chemosensory receptor family and raise the possibility that their ancestral role was in embryonic development.

¹Faculty of Biology and Medicine, Center for Integrative Genomics, University of Lausanne, Genopode Building, CH-1015 Lausanne, Switzerland. ²Sars Centre for Marine Molecular Biology, University of Bergen, Bergen N-5008, Norway. ³Departments of Genetics, Evolution and Environment, and Cell and Developmental Biology, University College London, London WC1E 6BT, UK. † Present address: Developmental Biology Unit, Observatoire Océanologique, 06234 Villefranche-sur-mer, France. Correspondence and requests for materials should be addressed to P.O. (email: P.Oliveri@ucl.ac.uk), F.R. (email: Fabian.Rentzsch@sars.uib.no) or to R.B. (email: Richard.Benton@unil.ch).

The insect chemosensory receptor superfamily, including gustatory receptors (GRs) and odorant receptors (ORs) (which represent an expanded clade within the GR family¹), are polytopic membrane proteins responsible for detecting a vast number of non-volatile and volatile chemicals in the environment^{2,3}. Most sequenced insect genomes are predicted to encode several dozen to a few hundred highly divergent GRs and/or ORs⁴. Almost all of these receptors are likely to be expressed in small subsets of sensory neurons in peripheral chemosensory organs. Here they recognize external chemical cues—including esters, alcohols, ketones and volatile lipid-derived pheromones (for ORs), and sugars, bitter compounds and cuticular pheromones (for GRs)—to permit perception of food, environmental dangers, kin and potential mates^{5,6}. A few exceptional GRs have either internal chemosensing or other sensory functions^{7–9}. In the presence of their cognate ligands, these receptors induce neuronal firing, although their signalling mechanism is poorly understood. ORs are thought to function as odour-gated ion channels^{10,11}, formed by a complex of an odour-specific OR and a co-receptor, ORCO¹². GRs are less well characterized molecularly: although they are also likely to function ionotropically¹³, it remains unclear whether they function alone or in complexes of co-expressed GR subunits¹⁴.

Understanding the molecular mechanism by which GRs and ORs act has been hampered by their lack of sequence similarity to either known ion channels or other types of membrane protein. The receptors are predicted to contain seven transmembrane domains (TMDs), similar to G protein-coupled receptors (GPCRs). Their membrane topology is, however, inverted compared with GPCRs, defining them as a distinct class of transmembrane protein^{12,15,16}. Thus, despite the widespread function for insect chemosensory receptors in mediating perception of the external chemical world, the genesis of this protein family is unknown.

In this work, we have used comparative genomics to characterize the evolutionary origins and dynamics of this family of receptors, and experimental analyses of GR homologues in species distant from insects to reveal an unexpected role for these proteins during embryonic development.

Results

Deep conservation of *Grl* genes. We performed TBLASTN and PSI-BLAST searches using insect GRs and ORs as queries to identify putative homologous genes within non-insect genomes available at NCBI and other public genome and Expressed Sequence Tag (EST) databases (see Methods) (Fig. 1a, Supplementary Table 1 and Supplementary Data 1). Within Protostomia, these searches recovered the previously described GRs of the crustacean *Daphnia pulex* (water flea)¹⁷, and the gustatory related (*gur*) and serpentine receptor class R (*srr*) genes of *Caenorhabditis elegans*^{1,18,19} and other nematodes. Beyond Ecdysozoa, we identified what we term GR-like (*Grl*) genes in Lophotrochozoa, including the annelids *Capitella teleta* (polychaete worm) and *Helobdella robusta* (freshwater leech)²⁰, and the molluscs, *Lottia gigantea* (owl limpet)²⁰, *Crassostrea gigas* (Pacific oyster)²¹ and *Aplysia californica* (sea slug). We also found homologous genes in Deuterostomia, including the hemichordate *Saccoglossus kowalevskii* (acorn worm), and several echinoderms, including the sea urchin *S. purpuratus*²², but not in any chordate (Fig. 1a). Finally, we identified a small number of *Grl* genes in non-bilaterian species, including Cnidaria, such as the sea anemone *N. vectensis*²³ (independently noted in another study²⁴), the corals *Acropora digitifera*²⁵ and *Acropora millepora*, and the placozoan *Trichoplax adhaerens*²⁶. However, no sequences were

recovered from the genomes of another cnidarian, *Hydra magnipapillata*, the ctenophores *Mnemiopsis leidyi*²⁷ and *Pleurobrachia bachei*²⁸, or the sponges *Amphimedon queenslandica*²⁹ and *Oscarella carmela*³⁰. No fungal, unicellular eukaryotic or prokaryotic genomes contained identifiable *Grls* (Fig. 1a).

Several observations support the classification of the identified genes as *Grls*. First, reciprocal BLAST with each *Grl* sequence against insect genomes identified an insect GR as the most significant hit. Second, the encoded proteins each contain multiple predicted TMDs—most commonly 6–7 TMDs in putative full-length *Grl* sequences—similar to GRs and ORs (Fig. 1b). (Accurate computational predictions of TMD number and topology are difficult because of the variable hydrophobicity of TMDs within this family of receptors¹²). Third, the phase and position of three inferred ancestral introns in the 3' region of *Drosophila melanogaster* GR transcripts¹ are well-conserved in *Grls* (Fig. 1c). Finally, *Grls* share a number of characteristic amino acid residues with the most highly conserved C-terminal region of the insect receptors, including a tyrosine residue important for ion channel function in insect ORs³¹ (Fig. 1c).

The overall sequence similarity of *Grls* and insect GRs (or ORs) is very low (~15%–20% amino acid identity, similar to the minimum identity within the GR and OR families themselves¹), with the highest similarity to the GR64a-f/GR61a clade of sugar-sensing receptors¹⁴. Phylogenetic analysis revealed no unambiguous orthologous relationships of *Grls* with any insect GR, or between *Grls* of different lophotrochozoan, deuterostome or non-bilaterian species (Fig. 2). Although the high divergence of these sequences precludes accurate reconstruction of their ancestry, many members of these repertoires appear to have formed by species-specific expansions (Fig. 2).

Early developmental expression of *Grl* genes in *N. vectensis*.

To investigate the role of *Grls* in non-Arthropoda, we focused in this study on the cnidarian *N. vectensis* (here abbreviated *Nvec*), which is amenable to gene expression and functional analyses. Moreover, the development and anatomy of this organism are relatively well-described, and a presumed chemosensory structure, the apical organ, has been identified (Fig. 3a)^{32,33}. *N. vectensis* development proceeds through a coeloblastula stage to gastrulation, which occurs mainly by invagination^{34,35}. After gastrulation, the embryo emerges from the egg jelly as a free-swimming planula, which moves by ciliary beating with the apical sense organ pointing forward. Subsequently, the planula transforms ('metamorphoses') into a sessile polyp, which starts feeding after formation of the tentacles that surround the single opening of the animal (Fig. 3a).

Surprisingly, analysis of the temporal pattern of expression of the two *Grls* we found in this species, *NvecGrl1* and *NvecGrl2*, by quantitative reverse transcriptase-PCR (qPCR) revealed the highest level of expression of these genes in early developmental stages (Fig. 3b and Supplementary Table 2): *NvecGrl1* is expressed in the egg and blastula, gastrula and early planula stages, diminishing rapidly to very low levels later in development (Supplementary Table 2). *NvecGrl2* is only robustly detected in the egg and blastula. These temporal expression profiles contrast markedly with those of *D. melanogaster* GRs and ORs, where expression of these receptors has been reported only in differentiated sensory neurons⁵.

We next examined the spatial distribution of *N. vectensis* *Grl* transcripts by whole-mount RNA *in situ* hybridization on a range of developmental stages. Although *NvecGrl2* RNA was undetectable in these experiments (Supplementary Fig. 1), we first

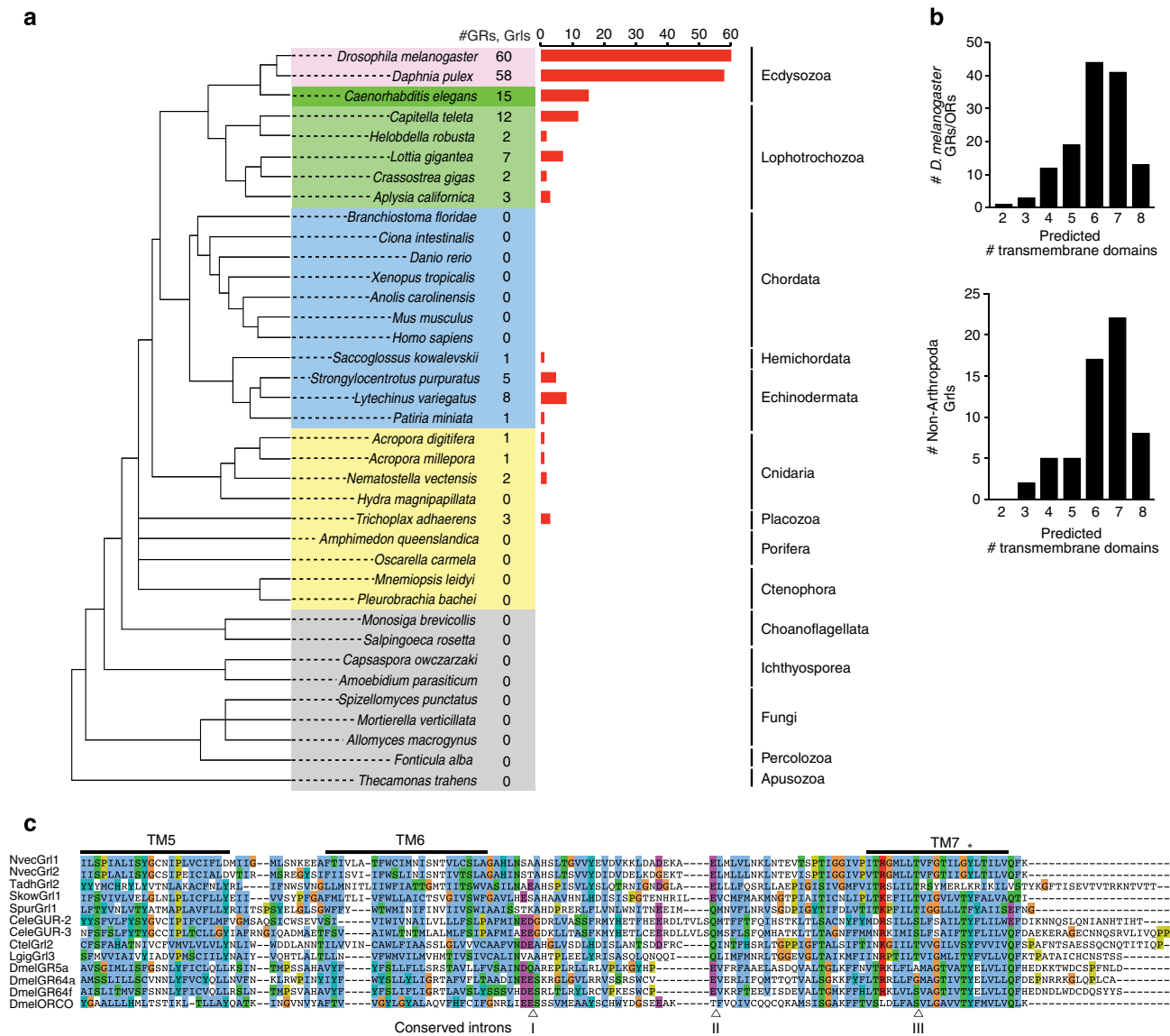


Figure 1 | Identification of *GrI* genes. (a) Summary of the *GR/GrI* repertoires identified in the genomes of selected arthropods (pink), non-arthropod Ecdysozoa (dark green), Lophotrochozoa (light green), Deuterostomia (blue) and non-Bilateria (yellow). An unscaled tree showing the phylogenetic relationships between these species is illustrated on the left; relationships among the different non-bilaterian phyla is unresolved, with the exception of the Cnidaria, which are the closest sister group to Bilateria⁶². Related genes were identified in multiple species of nematode worms but, for simplicity, only *C. elegans* is shown. (b) Computational predictions of the number of TMDs found in *D. melanogaster* GRs and ORs (top), and GrIs (bottom). *GrI* sequence fragments (lacking start/stop codons) were excluded from this analysis. (c) Alignment of the C-terminal regions of select insect GRs and ORs, *C. elegans* GURs and GrIs. Predicted TMDs are indicated with horizontal lines. The asterisk marks a conserved tyrosine residue important for ion conduction in insect ORs³¹. The arrowheads below the alignment indicate the positions of three phase 0 ancestral GR introns (inferred from analysis of *D. melanogaster* GRs and ORs) that are conserved in *GrIs*: intron I is conserved in phase and position in *NvecGrI1*, *NvecGrI2*, *TadhGrI2*, *SpurGrI1*, *CeleGUR-2*, *CeleGUR-3*, *CtelGrI2* and *LgigGrI3*; intron II is conserved in phase and position in *NvecGrI1*, *NvecGrI2*, *TadhGrI2*, *SpurGrI1*, *CtelGrI2* and *LgigGrI3*. Intron III is conserved in all sequences.

observed *NvecGrI1* transcripts in a broad aboral domain at the gastrula stage (Fig. 3c). This domain develops under the control of genes homologous to those that regulate anterior (or apical) development in bilaterians³⁶, and its centre is the site of formation of the apical sensory organ in the planula larva (Fig. 3a). Genes with similarly broad aboral expression at the gastrula stage display different expression dynamics after gastrulation: ‘spot genes’ (for example, *NvecFgfa1*, *NvecFgfa2* and *NvecSoxB1*) become restricted to a small spot at the aboral pole, from which the apical organ develops, whereas ‘ring genes’ (for example, *NvecSix3/6* and *NvecFoxQ2a*) remain expressed in a ring-like domain around the apical organ³⁶. Comparison of the spatial distribution of *NvecGrI1* with *NvecFGFa1* by double RNA

in situ hybridization revealed that the *NvecGrI1* expression domain remains broad at late gastrula/early planula stages when *NvecFgfa1* has already restricted to a small aboral spot (Fig. 3d). Subsequently, *NvecGrI1* transcripts are excluded from the apical organ-forming spot (Fig. 3e), similar to other ‘ring genes’. Although the ‘ring gene’ domain includes some scattered sensory cells^{37,38}, the broad and early expression of *NvecGrI1* in the aboral domain indicates that this receptor may primarily have a non-chemosensory role in this species.

Regulation of *NvecGrI1* by the aboral patterning network. Several transcription factors and signalling molecules that are

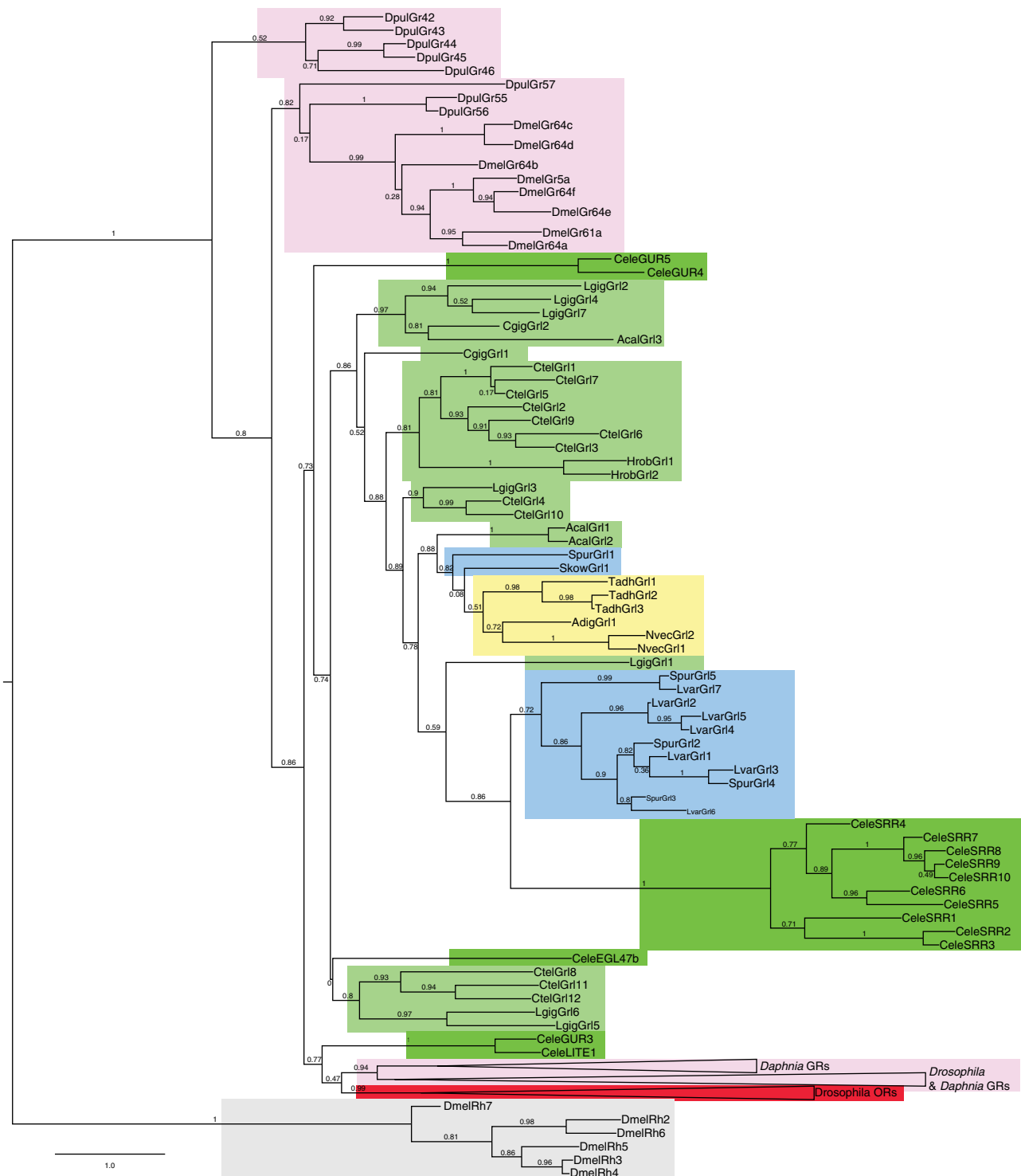


Figure 2 | Phylogenetic analysis of GrI, GR and OR genes. Maximum likelihood tree showing the relationships between select arthropod GRs/ORs, *C. elegans* GURs and all GrIs (except the short sequence fragments predicted in *P. miniata* and *A. millepora*), colour coded as in Fig. 1a. *Drosophila* Rhodopsins are included as an outgroup; although it remains unclear whether these two different families of heptahelical membrane proteins share a common ancestor, they clearly belong to a separate clade. For clarity, branches for large clades of *D. melanogaster* GRs/ORs or *D. pulex* GRs have been collapsed. The scale bar represents the number of amino acid substitutions per site.

expressed in the aboral region and required for apical organ formation in *N. vectensis* have been identified³⁶. For example, the homeodomain transcription factor *NvecSix3/6* is an important determinant of the aboral territory, where it initiates an autoregulatory loop of fibroblast growth factor (FGF) signalling to pattern this domain³⁶. To determine whether *NvecGr11* aboral

expression is regulated by these factors, we performed RNA *in situ* hybridization on embryos injected with morpholino oligonucleotides (morphants) designed to block translation of these genes. In *NvecSix3/6* morphants, *NvecGr11* aboral expression is reduced or absent in gastrula embryos compared with control morphants, similar to other markers of this

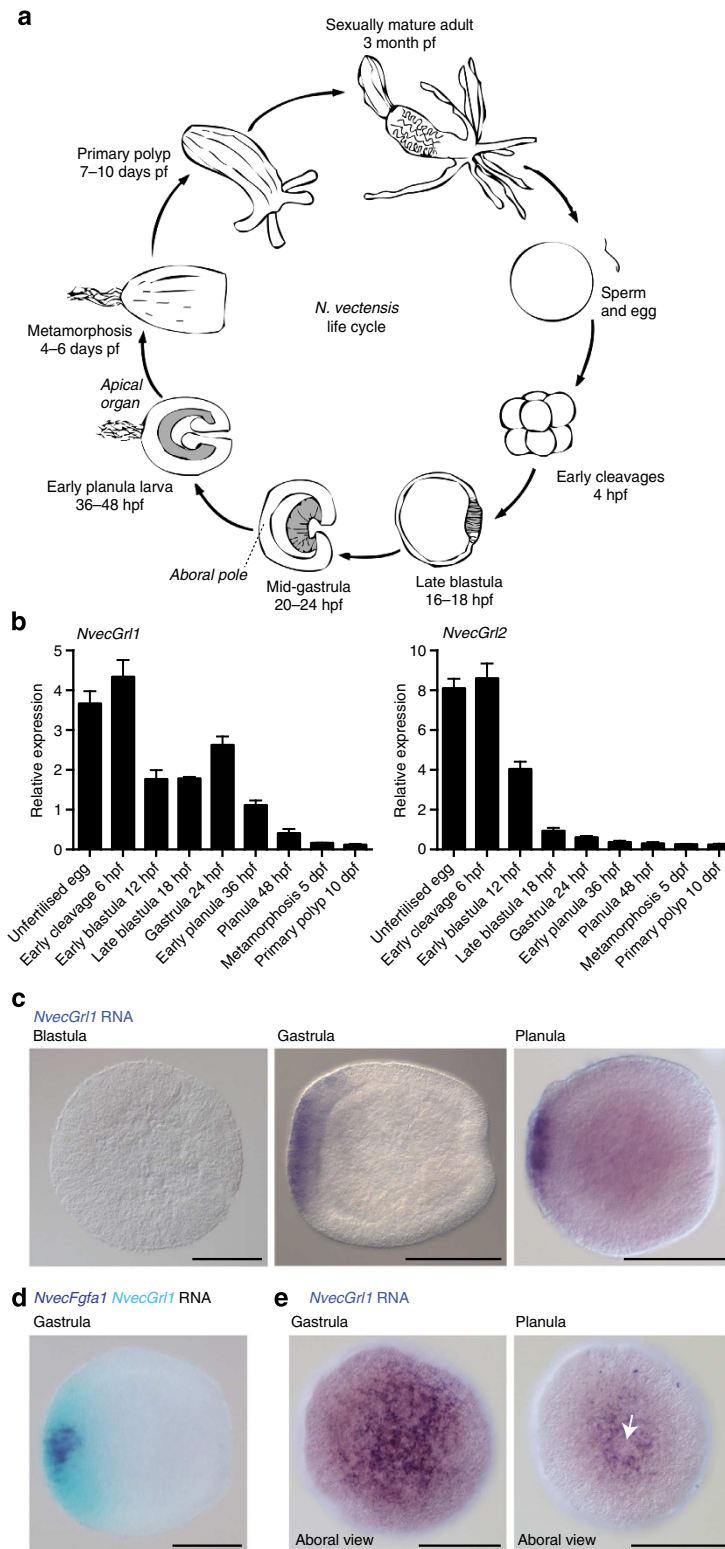


Figure 3 | *N. vectensis* Grls are expressed during early development. (a) Schematic of the life cycle of the sea anemone *N. vectensis*. Dark grey shading in the blastula, gastrula and early planula stages indicates the endoderm. Different stages are not drawn to scale; hpf = hours post-fertilisation. (b) Quantitative reverse transcriptase-PCR analysis of the temporal expression of *NvecGrl1* and *NvecGrl2* during nine developmental time points. Data from three biological replicate samples (mean \pm s.e.m.) are shown. (c) RNA in situ hybridization using a riboprobe against *NvecGrl1* on whole-mount *N. vectensis* at three developmental stages. Lateral views, with the aboral side on the left, are shown for all specimens in this and subsequent figures, unless otherwise noted. (d) Two-colour RNA in situ hybridization using riboprobes against *NvecGrl1* (light blue) and *NvecFgf1* (dark blue) on whole-mount *N. vectensis* embryos. (e) RNA in situ hybridization using a riboprobe against *NvecGrl1* on whole-mount *N. vectensis* at two developmental stages showing an aboral view, which reveal the formation of a ring-like distribution of transcripts at the planula stage. The apical organ forms from the unstained cells inside the ring (white arrow). Scale bars, 100 μ m (c–e).

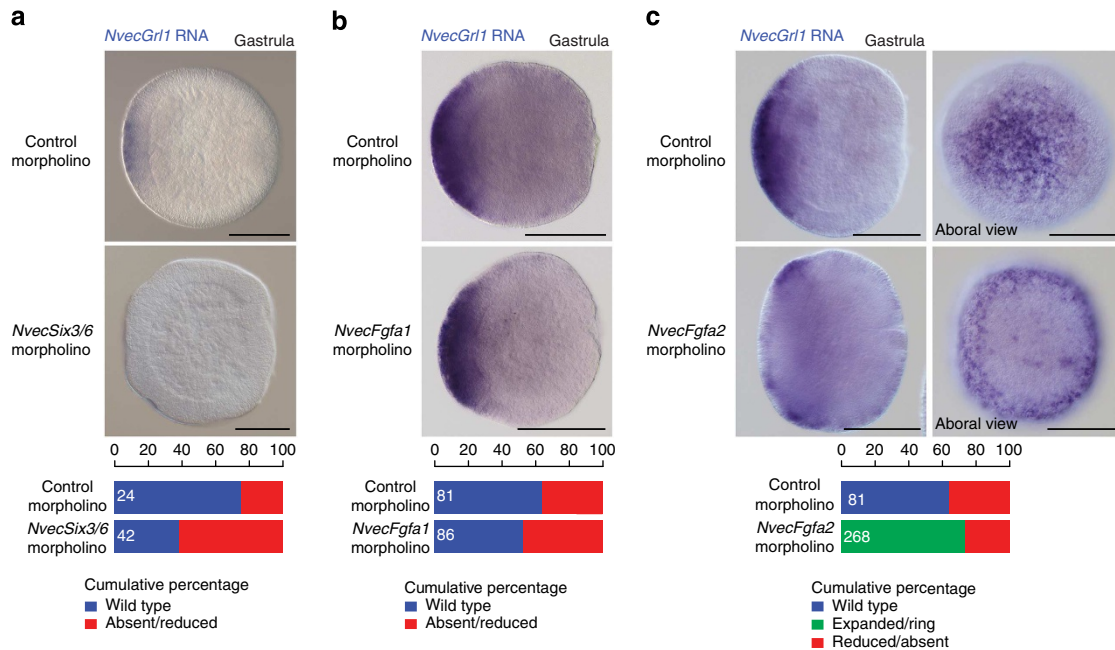


Figure 4 | Regulation of *N. vectensis* *Gr1* expression by the apical patterning network. (a) RNA in situ hybridization using a riboprobe against *NvecGr1* on whole-mount *N. vectensis* embryos injected with either control or *NvecSix3/6* morpholino oligonucleotides. Quantification of the phenotypes is shown below. Note that *NvecGr1* transcripts are relatively weakly detected and a fraction of control morpholino-injected animals did not exhibit staining. The *n* is shown in white within each bar in this and all equivalent graphs. **(b)** RNA in situ hybridization using a riboprobe against *NvecGr1* on whole-mount *N. vectensis* embryos injected with either control or *NvecFgfa1* morpholino oligonucleotides. Quantification of the phenotypes is shown below. **(c)** RNA in situ hybridization using a riboprobe against *NvecGr1* on whole-mount *N. vectensis* embryos injected with either control or *NvecFgfa2* morpholino oligonucleotides. In *NvecFgfa2* morphants, note the precocious formation and larger size of the ring of *NvecGr1* transcripts around the aboral pole (compare with Fig. 3e). Quantification of the phenotypes is shown below. Scale bars, 100 μ m (a–c).

domain³⁶ (Fig. 4a), suggesting that *NvecGr1* functions downstream of this transcription factor.

NvecFgfa1 and *NvecFgfa2* participate in positive and negative feedback regulation of apical organ formation, respectively^{33,36}. *NvecFgfa1* morphants fail to develop an apical organ³³, whereas *NvecFgfa2* morphants display precocious formation of an expanded apical organ³⁶. However, although effects of *NvecFgfa1* knockdown become visible only after gastrulation, an expansion and/or upregulation of apical organ domain genes in *NvecFgfa2* knockdown animals is detectable already at gastrula stage³⁶. Consistently, we found that the expression of *NvecGr1* appears only slightly affected in *NvecFgfa1* morphants at the end of gastrulation (Fig. 4b). By contrast, in *NvecFgfa2* morphants, *NvecGr1* expression forms an expanded ring with a wider area of low *NvecGr1* expression in its centre and this ring-like domain appears earlier than in control animals (Fig. 4c compared with Fig. 3e). These data provide further evidence that *NvecGr1* is expressed in cells that do not directly give rise to the apical sensory organ.

***Gr1* is required for aboral patterning in *N. vectensis*.** To investigate the function of *NvecGr1*, we injected zygotes with morpholino oligonucleotides designed to block translation of this receptor, and examined development of these animals in parallel with those injected with control morpholinos (see Methods). Early developmental processes, including gastrulation, appeared to proceed normally in both *NvecGr1* and control morphant animals (Fig. 5a). However, *NvecGr1* morphants displayed pronounced morphological defects in the apical organ domain in planula larvae (Fig. 5a,b). In control animals, the first sign of apical organ formation is the translocation of the nuclei in a small group of cells at the aboral pole to a more basal position (Fig. 5a).

These cells subsequently form a small indentation of the aboral ectoderm (Fig. 5a); this indentation is the site from which the long cilia of the apical organ emerge³⁷. In *NvecGr1* morphants, the initial basal movement of nuclei is absent or strongly reduced, and no clear indentation develops (Fig. 5a). Correspondingly, the apical tuft is absent or consists of only few long cilia in 4-day-old *NvecGr1* morphants (Fig. 5b). These animals subsequently fail to develop into primary polyps (0%, *n* = 159 *NvecGr1* morphants, compared with control morphants 63%, *n* = 122). These defects were reproduced with a second morpholino against *NvecGr1* (<9% primary polyps, *n* = 109).

To understand the basis for these morphological defects, we analysed expression of aboral domain patterning genes in *NvecGr1* morphants. *NvecSix3/6* expression is greatly diminished—but not abolished—in *NvecGr1* morphants at the planula stage compared with control morphants (Fig. 5c). Consistent with the reduction of *NvecSix3/6* expression, two of its downstream targets, the transcription factor *NvecFoxQ2a* and *NvecFgfa2* (ref. 36), are also reduced in *NvecGr1* morphants compared with controls (Fig. 5c). Defects in gene expression were also detectable at gastrula stages (Supplementary Fig. 2a), when *NvecGr1* transcripts are first detected in the aboral domain, although these phenotypes were very subtle, though consistent, for *NvecSix3/6* and *NvecFoxQ2a*. Together, these observations implicate *NvecGr1* in a feedback pathway that maintains *NvecSix3/6* expression to pattern the aboral domain. By contrast, patterning genes expressed elsewhere in the embryo, for example, *NvecWnt2*, which is found in a belt-like domain between the aboral and oral poles³⁹, are not or at most mildly affected in *NvecGr1* morphants (Fig. 5c).

One of the important functions of the FGF signalling loop is to downregulate *NvecSix3/6* expression after gastrulation in a small ‘spot’, the developing apical organ domain. Within this spot,

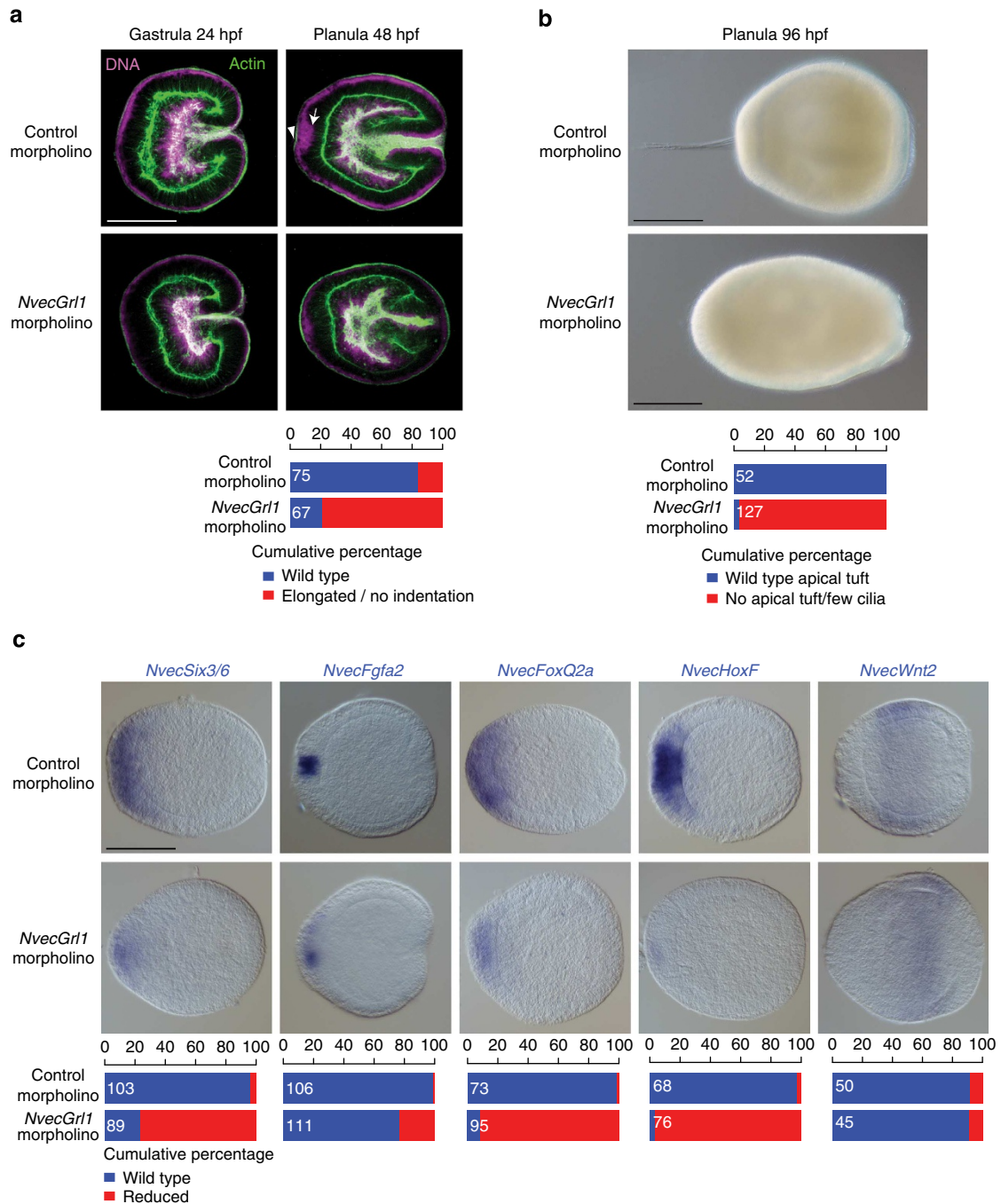


Figure 5 | *N. vectensis* Grl1 is required for aboral pole patterning. (a) Morphological phenotypes of *N. vectensis* embryos injected with either control (control#1) or *NvecGr1* (*NvecGr1*#1) morpholino oligonucleotides, in which DNA (magenta) and the actin cytoskeleton (green) are labelled with TO-PRO-3 and Alexa Fluor 488 Phalloidin, respectively. The arrow marks the group of nuclei at the aboral pole that have translocated to a more basal position (towards the right of the image) in control but not *NvecGr1* morphants; this results in these cells forming a small indentation of the apical ectoderm (arrowhead). Scale bar, 100 μ m (applies to all images). Quantification of the phenotypes is shown below. (b) Bright-field images of living 4-day planulae derived from *N. vectensis* embryos injected with either control (control#1) or *NvecGr1* (*NvecGr1*#2) morpholino oligonucleotides revealing the failure in apical tuft develops in *NvecGr1* morphants. Quantification of the phenotypes is shown below. Scale bars, 100 μ m. (c) RNA in situ hybridization using probes against marker genes in animals injected with either control (control#1) or *NvecGr1* (*NvecGr1*#1) morpholino oligonucleotides. Scale bar, 100 μ m (applies to all images). Quantification of the phenotypes is shown below.

genes required for apical organ formation, such as the transcription factor *NvecHoxF*, are expressed³⁶. Defects in the initiation of FGF signalling leads to a failure in formation of this *NvecSix3/6*- and *NvecFoxQ2a*-negative and *NvecHoxF*-positive aboral spot³⁶. We observed a similar phenotype in *NvecGr1*, but not control,

morphants (Fig. 5c and Supplementary Fig. 2b); these defects could account for failure of apical organ development. Together, these results support a role for *NvecGr1* in the regulatory network that controls aboral domain patterning and thereby apical sensory organ formation.

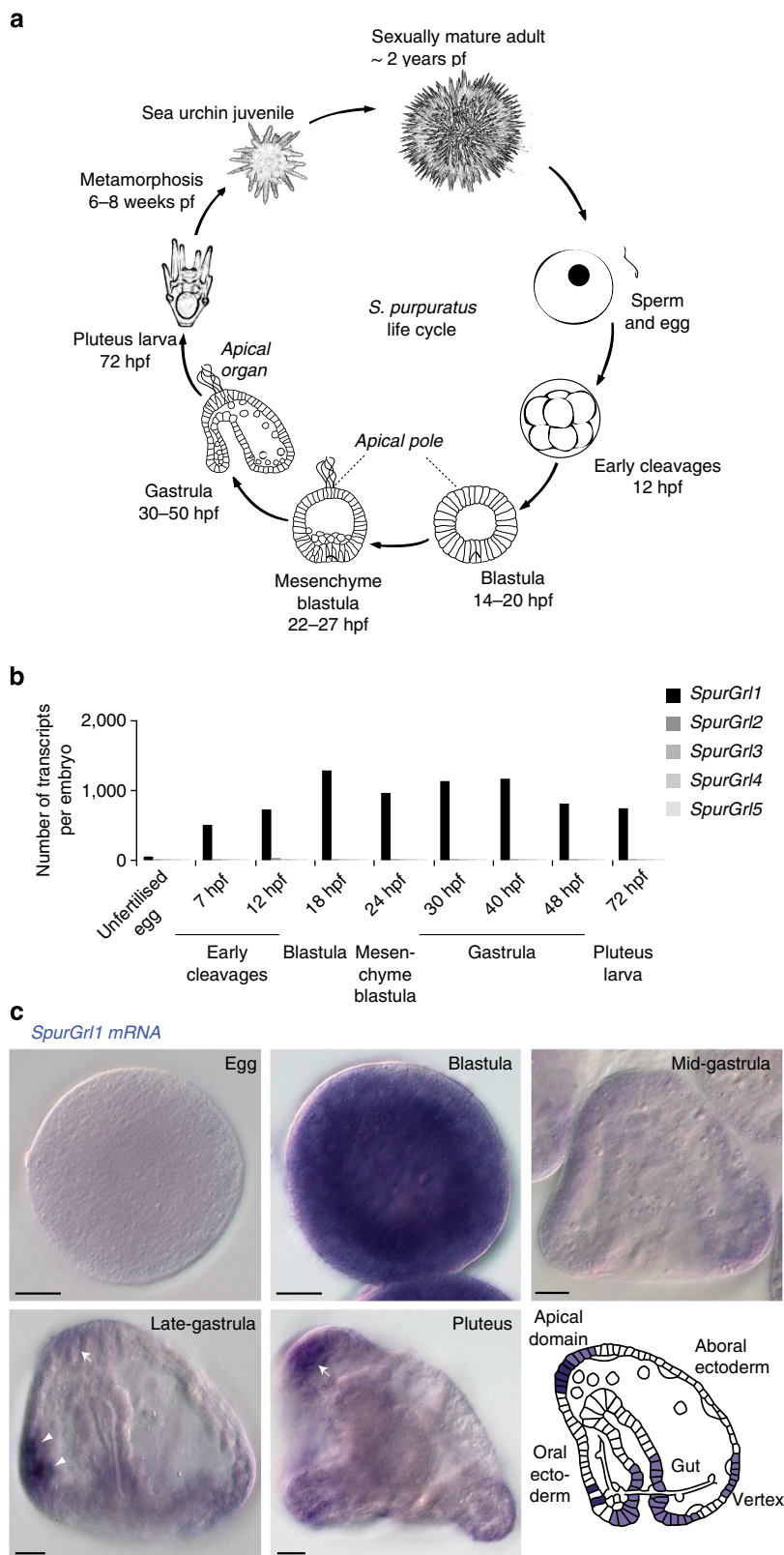


Figure 6 | Early developmental expression of an *S. purpuratus* Gr1. (a) Schematic of the life cycle of the sea urchin *S. purpuratus*. (b) Quantitative reverse transcriptase-PCR analysis of the temporal expression of the five *SpurGr1* genes during nine developmental time points. Data are represented as number of transcripts per embryo and represent the average of four technical replicates in each of two independent biological replicate samples (see Supplementary Table 3). (c) RNA in situ hybridization using a riboprobe against *SpurGr1* on whole-mount *S. purpuratus* of five developmental stages. All the embryos represent lateral views: as indicated in the schematic, the oral ectoderm is on the left and the apical domain on the top in the gastrula and pluteus specimens. The arrows mark the expression of *SpurGr1* in the apical domain (where the apical organ will form), while the arrowheads mark a pair of presumptive neurosecretory cells in the oral ectoderm. Scale bars, 20 μ m.

Developmental expression of a deuterostome *Grl* gene. To determine whether the early developmental expression of *Grl* genes is conserved in Deuterostomia, we used qPCR to analyse transcript levels of the five *Grls* of the echinoderm *S. purpuratus* during embryonic stages (Fig. 6a). Notably, *SpurGrl1*, which is the most similar sea urchin *Grl* to *NvecGrl1* (Fig. 2), was detected during early development (Fig. 6b and Supplementary Table 3): the highest expression of *SpurGrl1* was at the blastula stage, but it remained at elevated levels in the gastrula and later embryonic developmental stages. These qPCR data are in agreement with quantitative developmental transcriptome data (Supplementary Fig. 3a)⁴⁰. The other four *SpurGrls* were expressed at only very low levels during developmental stages (Fig. 6b), but transcripts could be readily amplified for all *SpurGrls*, except *SpurGrl3*, from adult neural tissue (Supplementary Fig. 3b). These observations suggest that *SpurGrl1* has a unique function during embryonic development.

By whole-mount RNA *in situ* hybridization, we observed that *SpurGrl1* exhibits a dynamic spatial expression pattern during early development (Fig. 6c). In the blastula *SpurGrl1* RNA was present ubiquitously, while in later stages it was restricted to a few groups of cells. From the late gastrula, transcripts were detected in cells in the apical domain, which develops into a neurosensory structure⁴¹. Strong *SpurGrl1* expression was also detected in two bilaterally arrayed cells in the oral ectoderm and, at lower levels, in the hindgut and adjacent ectoderm, as well as a region of the aboral ectoderm that will develop into the vertex (Fig. 6c). The apical domain expression of *SpurGrl1* represents an intriguing parallel with that of *NvecGrl1* in the developmentally equivalent region of the sea anemone gastrula^{36,42,43}, although the additional expression patterns suggest that the sea urchin gene has several functions.

Discussion

We have defined an early evolutionary origin and broad phylogenetic distribution of the insect chemosensory receptor superfamily. Previously only characterized in Ecdysozoa^{2,17,44,45}, we show *Grl* genes are present in genomes across Protostomia, non-chordate Deuterostomia and non-Bilateria. These observations establish the origin of this gene family before the split of Bilateria and non-Bilateria 550–850 million years ago⁴⁶, and suggest that these genes have been lost in the ancestral chordate.

Through analysis of *Grls* in the non-bilateria *N. vectensis*, we found—unexpectedly—several lines of evidence supporting a role in developmental body patterning rather than external chemosensation. First, the existence of a small number of *NvecGrls* is inconsistent with this cnidarian receptor repertoire playing a wide-ranging role in the detection of environmental chemical signals. We note that *N. vectensis* has several dozen vertebrate OR-like GPCRs, which represent candidate chemosensory receptors of this species⁴⁷. Second, in contrast to *Drosophila* ORs and GRs⁴⁸, both *NvecGrls* are expressed in early developmental stages, before formation of sensory neurons and a putative chemosensory organ (at late gastrula and mid-planula stage, respectively^{37,38}). Moreover, *NvecGrl1* transcripts are detected broadly around the aboral pole in gastrula and planula stages, but are selectively excluded from an aboral ‘spot’ of cells that subsequently gives rise to the apical sensory organ. Third, functional analysis of *NvecGrl1* supports a role in aboral body patterning essential for developmental progression. Although our data argue that *NvecGrls* have a different function to insect GRs, we cannot exclude that they have a later, additional role, for example, in the detection of metamorphosis-related sensory signals.

Although loss of *NvecGrl1* blocks developmental progression beyond the planula stage, the relatively limited current knowledge of aboral patterning in Cnidaria makes it difficult to define the precise role of this protein. Our data are consistent with a model in which *NvecGrl1* functions downstream of the aboral territory determinant *NvecSix3/6* in the feedback loop that is important to refine aboral pole patterning and promote apical organ formation³⁶. Secondary structure and sequence conservation of *NvecGrl1* (and other *Grls*) with insect GRs and ORs suggest that this protein acts as a ligand-gated ion channel and might recognize a paracrine developmental signal; testing this model will require identification of a relevant ligand. Nevertheless, it is intriguing that *NvecGrl1* plays a role in the formation (albeit indirectly) rather than the function of a putative chemosensory organ. We have not been able to detect transcripts for *NvecGrl2* gene *in situ* and morpholino-mediated knockdown of *NvecGrl2* did not reveal any obvious patterning defects (unpublished data), suggesting that this gene has a different role to *NvecGrl1*.

The similarities in the early developmental expression of the deuterostome *Grl* gene with highest sequence identity to *NvecGrl1*, *S. purpuratus Grl1*, hints that a role in embryonic patterning may have been an ancestral function of this family. However, *SpurGrl1* displays additional spatial expression patterns beyond the apical domain and four additional *SpurGrls* do not show such early expression, suggesting that *Grls* in this species have multiple different roles. Clearly dissecting the function of *SpurGrl1* (and its paralogues) will require methods that permit tissue-specific gene knockdown.

Beyond the work presented here, very little is known about the role of members of the GR/*Grl* family outside insects. The large size and high sequence divergence of the GR repertoire in the crustacean *D. pulex* is consistent with a role in chemosensation¹⁷, although no expression or functional analyses of these receptors have been reported. The nematode *C. elegans* relies on a very large family of GPCRs for chemical detection¹⁸, and of the 15 *Grl* genes (the *gur* and *srr* families^{1,18,19}, the latter not previously defined as members of this superfamily) only two have been characterized. GUR-2 (also known as LITE-1) functions in photosensitive neurons^{44,45}, although it has not been determined whether this protein senses light directly. GUR-1 (also known as EGL-47) appears to regulate motoneurons that control egg laying⁴⁹. Together with our data in *N. vectensis* and *S. purpuratus*, these observations suggest that *Grl/GR* genes may have been recruited only in arthropods to fulfil a predominant role in peripheral chemosensation. Future analysis of other *Grls* in a range of species should yield insights into the diverse functions and evolutionary history of this unusual receptor family.

Methods

Gene identification. To identify homologues of insect chemoreceptors, all known *Drosophila* sequences of GRs and ORs were used as queries in extensive TBLASTN and PSI-BLAST searches of public genome and EST data sets (see Supplementary Table 1 and Supplementary Data 1), and in screens of OrthoDB⁵⁰. Identified genes were used in iterative BLAST searches of species-specific data sets until no new sequences were identified. The numbers of genes in most species are likely to represent minimum estimates due to the challenge of identifying highly divergent *Grl* genes from incompletely assembled genomes with computational predictions alone. For the same reasons, most predicted sequences are incomplete, particularly at the more divergent 5' end. Analysis of the membrane topology (excluding partial protein sequences) was performed using TMHMM v.2.0 (ref. 51). Intron positions and phases were predicted by comparing cloned (or predicted) transcript sequences and the corresponding genomic sequences.

Alignment/phylogenetic tree building. Protein alignments were built using Clustal Omega⁵² with the following settings—max HMM Iterations: 5; combined iterations: 5; max guide iterations: 5. The amino termini of the sequences were cut off after aligning using Jalview⁵³ and only the carboxy-terminal regions from TMD5 (starting with position 352 in DmelORCO) was used for further analysis. Tree reconstruction was performed using PhyML3.0 (ref. 54) and the LG model⁵⁵

was used as a substitution matrix. Branch support was calculated using the approximate likelihood-ratio test method⁵⁶. The tree was rooted on the Rhodopsin branch, although we acknowledge that the evolutionary relationship between these receptor families is still unclear.

Cloning of full-length *Grl* coding sequences. To obtain the complete coding sequence of *NvecGrl1*, PCR was performed on mixed embryo stage complementary DNA, with specific primers based on EST and genome data (genome.jgi-psf.org/Nemve1/Nemve1.home.html). For *NvecGrl2* 5' and 3' rapid amplification of cDNA end (RACE) PCRs were performed. The following primer sets were used:

NvecGrl1: 5'-GTGTGAGCACGCTGCGAGAATGG-3'
3'-TCACTTAACTGGACAAGAATCG-5'
NvecGrl2: 5'RACE outer primer: 5'-AGAGCAGAAGGCTCACAAAGC-3'
5'RACE inner primer: 5'-CAAGGAATTTTCATTGCGACAG-3'
3'RACE outer primer: 5'-CGATTGGAGGAATTGTCCAGTAACACGCGG-3'
3'RACE inner primer: 5'-TCAACACAGAAGTGATCAGCCCAACGATTGG-3'
Genbank accession numbers are: KP294348 (*NvecGrl1*) and KP294349 (*NvecGrl2*).

For *SpurGrl1*, a 1,212 bp fragment of the coding sequence was amplified by PCR from 18 hpf embryonic cDNA, cloned into pGEM-T Easy (Promega) and sequenced, using the following primers designed on the WHL22.291934 transcriptome sequence:

5'-GAACACCACTCATGGAACC-3'
3'-CTATGGGATCACCGCTCACT-5'

Quantitative PCR. For *N. vectensis*, cell lysates of embryonic stages were collected and total RNA was extracted using the RNAqueous kit (Ambion). cDNA synthesis was performed using the SuperScript II RT Reagent Kit, according to the manufacturer's protocol. Expression of *NvecGrl1*, *NvecGrl2* and reference genes were analysed by performing PCR on an Applied Biosystems 7900HT SDS, using the cDNA as template and SYBR Premix (Roche) with the following primers:

NvecGrl1
5'-AATCGTGCTAGCCACATCTGGTG-3'
3'-ACCTCGTACACAACGCCTGTCAAA-5'
NvecGrl2
5'-ACTATAGTAACGTCACCTGCGGGTGC-3'
3'-TTCGCGCTCTTTCAGTTCATCCAC-5'
Ef1b
5'-TGCTGCATCAGAACAGAAACCTGC-3'
3'-TAAGCCTTCAAGCGTCTTGCCTG-5'
RibPrL23
5'-TTACGGAGCTCTGGCTTTCCTTTC-3'
3'-TGCCGTTAAGGGTATCAAAGGACG-5'

The reference target stability values were as follows EF1 α ($M = 0.404$; $CV = 0.135$), RibPr23L ($M = 0.404$; $C = 0.144$), average ($M = 0.404$; $CV = 0.140$).

For *S. purpuratus*, cell lysates of appropriately staged embryos were collected and total RNA was extracted using the RNeasy Micro Kit (Qiagen). cDNA synthesis was performed using the iScript cDNA Synthesis Kit (Bio-Rad), according to the manufacturer's instructions. At least four technical replicas were run on two independent cDNA batches, using cDNA equivalent to 1 embryo per reaction (2.8 ng) and Power SYBR Green QPCR master mix (Applied Biosystems), on the 7900HT Fast Real-Time PCR system and the following primers (*SpurUbg* was used as internal standard^{57,58}):

SpurGrl1
5'-TCTGCGAATCGAGAAGTCC-3'
3'-GAGCCATAGTCGCGTAGGTC-5'
SpurGrl2
5'-CATCCAGGCTGAAGACAA-3'
3'-GCAACTTGAAACGCCCATAC-5'
SpurGrl3
5'-GCCTCAATTTAGCGGCAGTA-3'
3'-CCAGATAGGATGTGGCAGGT-5'
SpurGrl4
5'-ATCCTCAGCCCTTCTGACA-3'
3'-GAACTGGTCGGTCAGGATGT-5'
SpurGrl5
5'-ATAACGCTGAGCCGGTACAA-3'
3'-TGGTTGCAGCAGTTTGAAG-5'
SpurUbg
5'-CACAGGCAAGACCATCACAC-3'
3'-GAGAGAGTGCAGCCATCCTC-5'

Morpholinos. Translation-blocking antisense morpholino oligonucleotides (GeneTools, LLC) were designed to match the sequence of *NvecGrl1*. The sequences of the morpholinos used are:

NvecGrl1#1: 5'-ACGCTCCGACTGGAATGCCATTCA-3'
NvecGrl1#2: 5'-GAACTGCCATTTCATCCGCTTGTTC-3'
control#1 (generic³⁶): 5'-CCATTGTGAAGTTAAACGATAGATC-3'
control#2 (*NvecGrl1* mismatch): 5'-ACGCGCCTACTGGAATTGCTATTAA-3'

The two morpholinos against *NvecGrl1* are partially overlapping to avoid 5'-untranslated region sequence that is present elsewhere in the genome. The sequence corresponding to the start codon in the *NvecGrl1* morpholinos is underlined.

Six3/6: 5'-GTACTGCCGCACTGCAAGACTGTGC-3' (ref. 36)
Egfa1: 5'-ATAAGGTGGACGCATGACTTTGTAG-3'
Egfa2: 5'-CGTTAGCATGGTGATCGTCATGTTG-3' (ref. 33)

***Nematostella* culture, manipulation and microinjection.** Animals were cultured at 18 °C in 1:3 diluted sea water in the Sars Centre Cnidaria facility, and gamete production was induced by overnight exposure to light and elevated temperature (25 °C)⁵⁹. Morpholinos were diluted in H₂O, together with a tracer (Alexa568 Dextran (Molecular Probes) at 0.1 mg ml⁻¹), to a final concentration of either 1 mM (*NvecGrl1*#1) or 0.6 mM (*NvecGrl1*#2); control morpholinos were diluted to the same concentration in parallel experiments. Zygotes were microinjected using an Eppendorf Femtojet, with a volume equivalent to ~5% of the egg. Following injections, the embryos were transferred to Petri dishes containing *Nematostella* medium and were allowed to develop at 21 °C until fixation. For images of live planulae, animals were mounted in 2% methylcellulose (in *Nematostella* medium) and imaged on a Nikon Eclipse E800 microscope.

Histology. *N. vectensis*. For actin and DNA staining, specimens were fixed in 4% formaldehyde in PBT (0.1% Triton X-100 in PBS) for 1 h and washed four times in PBT. 30 μ l of Alexa Fluor 488 Phalloidin (Molecular Probes) were put in an open Eppendorf tube for 30 min at room temperature, to let the solvent evaporate. The pellet was redissolved in 1.5 ml PBT and 1.5 μ l TO-PRO-3 Iodide (Molecular Probes) was added. The specimens were incubated for 2–3 h in this staining solution, washed five times with PBT and mounted in ProLong Gold (Life Technologies). RNA *in situ* hybridization on *N. vectensis* was performed using antisense digoxigenin-labelled probes against the open reading frame (ORF) of the desired genes essentially as described⁶⁰. In brief, hybridization was carried out at 60 °C for 60 h, and post-hybridization stringency washes were with 0.01 \times SSC. Anti-digoxigenin Fab fragments (Roche) were diluted 1:5,000 before detection by NBT/BCIP staining (Roche). For *N. vectensis* double *in situ* hybridization, digoxigenin-labelled *NvecGrl1* and fluorescein isothiocyanate-labelled *NvecEgfa1* probes complementary to the corresponding ORF were used. *NvecEgfa1* was detected by NBT/BCIP staining and *NvecGrl1* was detected using anti-DIG-POD and tyramide-based signal amplification (TSA plus DNP (AP) kit, Perkin Elmer), followed by anti-DNP-AP-mediated BCIP staining.

S. purpuratus. Specimens were fixed in 4% formaldehyde in MOPS buffer overnight at 4 °C, then washed several times in MOPS buffer and once in 70% ethanol. After rehydration in TBST, RNA *in situ* hybridization was performed using an antisense digoxigenin-labelled probe against the 1,212 bp fragment of the *SpurGrl1* ORF (see above) as described⁶¹. In brief, 0.05 ng μ l⁻¹ of probe was hybridized at 60 °C for 16 h. Post-hybridization stringency washes were with 0.1 \times SSC and 0.01 \times SSC. Anti-digoxigenin Fab fragments were diluted 1:2,000 before detection by NBT/BCIP staining.

References

- Robertson, H. M., Warr, C. G. & Carlson, J. R. Molecular evolution of the insect chemoreceptor gene superfamily in *Drosophila melanogaster*. *Proc. Natl Acad. Sci. USA* **100**(Suppl 2): 14537–14542 (2003).
- Hallem, E. A., Dahanukar, A. & Carlson, J. R. Insect odor and taste receptors. *Annu. Rev. Entomol.* **51**, 113–135 (2006).
- Benton, R. Chemical sensing in *Drosophila*. *Curr. Opin. Neurobiol.* **18**, 357–363 (2008).
- Nei, M., Niihura, Y. & Nozawa, M. The evolution of animal chemosensory receptor gene repertoires: roles of chance and necessity. *Nat. Rev. Genet.* **9**, 951–963 (2008).
- Vosshall, L. B. & Stocker, R. F. Molecular architecture of smell and taste in *Drosophila*. *Annu. Rev. Neurosci.* **30**, 505–533 (2007).
- Su, C. Y., Menz, K. & Carlson, J. R. Olfactory perception: receptors, cells, and circuits. *Cell* **139**, 45–59 (2009).
- Miyamoto, T., Slone, J., Song, X. & Amrein, H. A fructose receptor functions as a nutrient sensor in the *Drosophila* brain. *Cell* **151**, 1113–1125 (2012).
- Xiang, Y. *et al.* Light-avoidance-mediating photoreceptors tile the *Drosophila* larval body wall. *Nature* **468**, 921–926 (2010).
- Ni, L. *et al.* A gustatory receptor paralogue controls rapid warmth avoidance in *Drosophila*. *Nature* **500**, 580–584 (2013).
- Sato, K. *et al.* Insect olfactory receptors are heteromeric ligand-gated ion channels. *Nature* **452**, 1002–1006 (2008).
- Wicher, D. *et al.* *Drosophila* odorant receptors are both ligand-gated and cyclic-nucleotide-activated cation channels. *Nature* **452**, 1007–1011 (2008).
- Benton, R., Sachse, S., Michnick, S. W. & Vosshall, L. B. Atypical membrane topology and heteromeric function of *Drosophila* odorant receptors *in vivo*. *PLOS Biol.* **4**, e20 (2006).

13. Sato, K., Tanaka, K. & Touhara, K. Sugar-regulated cation channel formed by an insect gustatory receptor. *Proc. Natl Acad. Sci. USA* **108**, 11680–11685 (2011).
14. Montell, C. A taste of the *Drosophila* gustatory receptors. *Curr. Opin. Neurobiol.* **19**, 345–353 (2009).
15. Zhang, H. J. *et al.* Topological and functional characterization of an insect gustatory receptor. *PLoS One* **6**, e24111 (2011).
16. Lundin, C. *et al.* Membrane topology of the *Drosophila* OR83b odorant receptor. *FEBS Lett.* **581**, 5601–5604 (2007).
17. Penalva-Arana, D. C., Lynch, M. & Robertson, H. M. The chemoreceptor genes of the waterflea *Daphnia pulex*: many Grs but no Ors. *BMC Evol. Biol.* **9**, 79 (2009).
18. Thomas, J. H. & Robertson, H. M. The *Caenorhabditis* chemoreceptor gene families. *BMC Biol.* **6**, 42 (2008).
19. Robertson, H. M. & Thomas, J. H. In *The C. elegans Research Community, WormBook* (ed. WormBook). doi: 10.1895/wormbook.1.7.1; <http://www.wormbook.org> (2006).
20. Simakov, O. *et al.* Insights into bilaterian evolution from three spiralian genomes. *Nature* **493**, 526–531 (2013).
21. Zhang, G. *et al.* The oyster genome reveals stress adaptation and complexity of shell formation. *Nature* **490**, 49–54 (2012).
22. Sodergren, E. *et al.* The genome of the sea urchin *Strongylocentrotus purpuratus*. *Science* **314**, 941–952 (2006).
23. Putnam, N. H. *et al.* Sea anemone genome reveals ancestral eumetazoan gene repertoire and genomic organization. *Science* **317**, 86–94 (2007).
24. Nordstrom, K. J., Sallman Almen, M., Edstam, M. M., Fredriksson, R. & Skioth, H. B. Independent HHsearch, Needleman--Wunsch-based, and motif analyses reveal the overall hierarchy for most of the G protein-coupled receptor families. *Mol. Biol. Evol.* **28**, 2471–2480 (2011).
25. Shinzato, C. *et al.* Using the *Acropora digitifera* genome to understand coral responses to environmental change. *Nature* **476**, 320–323 (2011).
26. Srivastava, M. *et al.* The *Trichoplax* genome and the nature of placozoans. *Nature* **454**, 955–960 (2008).
27. Ryan, J. F. *et al.* The genome of the ctenophore *Mnemiopsis leidyi* and its implications for cell type evolution. *Science* **342**, 1242592 (2013).
28. Moroz, L. L. *et al.* The ctenophore genome and the evolutionary origins of neural systems. *Nature* **510**, 109–114 (2014).
29. Srivastava, M. *et al.* The *Amphimedon queenslandica* genome and the evolution of animal complexity. *Nature* **466**, 720–726 (2010).
30. Nichols, S. A., Roberts, B. W., Richter, D. J., Fairclough, S. R. & King, N. Origin of metazoan cadherin diversity and the antiquity of the classical cadherin/beta-catenin complex. *Proc. Natl Acad. Sci. USA* **109**, 13046–13051 (2012).
31. Nakagawa, T., Pellegrino, M., Sato, K., Voshall, L. B. & Touhara, K. Amino acid residues contributing to function of the heteromeric insect olfactory receptor complex. *PLoS One* **7**, e32372 (2012).
32. Darling, J. A. *et al.* Rising starlet: the starlet sea anemone, *Nematostella vectensis*. *Bioessays* **27**, 211–221 (2005).
33. Rentzsch, F., Fritzenwanker, J. H., Scholz, C. B. & Technau, U. FGF signalling controls formation of the apical sensory organ in the cnidarian *Nematostella vectensis*. *Development* **135**, 1761–1769 (2008).
34. Magie, C. R., Daly, M. & Martindale, M. Q. Gastrulation in the cnidarian *Nematostella vectensis* occurs via invagination not ingression. *Dev. Biol.* **305**, 483–497 (2007).
35. Kraus, Y. & Technau, U. Gastrulation in the sea anemone *Nematostella vectensis* occurs by invagination and immigration: an ultrastructural study. *Dev. Genes Evol.* **216**, 119–132 (2006).
36. Sinigaglia, C., Busengdal, H., Leclere, L., Technau, U. & Rentzsch, F. The bilaterian head patterning gene *six3/6* controls aboral domain development in a cnidarian. *PLoS Biol.* **11**, e1001488 (2013).
37. Nakanishi, N., Renfer, E., Technau, U. & Rentzsch, F. Nervous systems of the sea anemone *Nematostella vectensis* are generated by ectoderm and endoderm and shaped by distinct mechanisms. *Development* **139**, 347–357 (2012).
38. Richards, G. S. & Rentzsch, F. Transgenic analysis of a *soxB* gene reveals neural progenitor cells in the cnidarian *Nematostella vectensis*. *Development* **141**, 4681–4689 (2014).
39. Kusserow, A. *et al.* Unexpected complexity of the Wnt gene family in a sea anemone. *Nature* **433**, 156–160 (2005).
40. Tu, Q., Cameron, R. A., Worley, K. C., Gibbs, R. A. & Davidson, E. H. Gene structure in the sea urchin *Strongylocentrotus purpuratus* based on transcriptome analysis. *Genome Res.* **22**, 2079–2087 (2012).
41. Burke, R. D. *et al.* A genomic view of the sea urchin nervous system. *Dev. Biol.* **300**, 434–460 (2006).
42. Marlow, H. *et al.* Larval body patterning and apical organs are conserved in animal evolution. *BMC Biol.* **12**, 7 (2014).
43. Santagata, S., Resh, C., Hejnol, A., Martindale, M. Q. & Passamanek, Y. J. Development of the larval anterior neurogenic domains of *Terebratalia transversa* (Brachiopoda) provides insights into the diversification of larval apical organs and the spiralian nervous system. *Evodevo* **3**, 3 (2012).
44. Liu, J. *et al.* *C. elegans* phototransduction requires a G protein-dependent cGMP pathway and a taste receptor homolog. *Nat. Neurosci.* **13**, 715–722 (2010).
45. Edwards, S. L. *et al.* A novel molecular solution for ultraviolet light detection in *Caenorhabditis elegans*. *PLoS Biol.* **6**, e198 (2008).
46. Hedges, S. B., Dudley, J. & Kumar, S. TimeTree: a public knowledge-base of divergence times among organisms. *Bioinformatics* **22**, 2971–2972 (2006).
47. Churcher, A. M. & Taylor, J. S. The antiquity of chordate odorant receptors is revealed by the discovery of orthologs in the cnidarian *Nematostella vectensis*. *Genome Biol. Evol.* **3**, 36–43 (2011).
48. Roy, S. *et al.* Identification of functional elements and regulatory circuits by *Drosophila* modENCODE. *Science* **330**, 1787–1797 (2010).
49. Moresco, J. J. & Koelle, M. R. Activation of EGL-47, a Galphao-coupled receptor, inhibits function of hermaphrodite-specific motor neurons to regulate *Caenorhabditis elegans* egg-laying behavior. *J Neurosci.* **24**, 8522–8530 (2004).
50. Waterhouse, R. M., Tegenfeldt, F., Li, J., Zdobnov, E. M. & Kriventseva, E. V. OrthoDB: a hierarchical catalog of animal, fungal and bacterial orthologs. *Nucleic Acids Res.* **41**, D358–D365 (2013).
51. Krogh, A., Larsson, B., von Heijne, G. & Sonnhammer, E. L. Predicting transmembrane protein topology with a hidden Markov model: application to complete genomes. *J. Mol. Biol.* **305**, 567–580 (2001).
52. Sievers, F. *et al.* Fast, scalable generation of high-quality protein multiple sequence alignments using Clustal Omega. *Mol. Syst. Biol.* **7**, 539 (2011).
53. Waterhouse, A. M., Procter, J. B., Martin, D. M., Clamp, M. & Barton, G. J. Jalview Version 2—a multiple sequence alignment editor and analysis workbench. *Bioinformatics* **25**, 1189–1191 (2009).
54. Guindon, S. *et al.* New algorithms and methods to estimate maximum-likelihood phylogenies: assessing the performance of PhyML 3.0. *Syst. Biol.* **59**, 307–321 (2010).
55. Le, S. Q. & Gascuel, O. An improved general amino acid replacement matrix. *Mol. Biol. Evol.* **25**, 1307–1320 (2008).
56. Anisimova, M. & Gascuel, O. Approximate likelihood-ratio test for branches: a fast, accurate, and powerful alternative. *Syst. Biol.* **55**, 539–552 (2006).
57. Oliveri, P., Carrick, D. M. & Davidson, E. H. A regulatory gene network that directs micromere specification in the sea urchin embryo. *Dev. Biol.* **246**, 209–228 (2002).
58. Rast, J. P. *et al.* Recovery of developmentally defined gene sets from high-density cDNA macroarrays. *Dev. Biol.* **228**, 270–286 (2000).
59. Fritzenwanker, J. H. & Technau, U. Induction of gametogenesis in the basal cnidarian *Nematostella vectensis* (Anthozoa). *Dev. Genes Evol.* **212**, 99–103 (2002).
60. Saina, M. & Technau, U. Characterization of myostatin/gdf8/11 in the starlet sea anemone *Nematostella vectensis*. *J. Exp. Zool. B Mol. Dev. Evol.* **312**, 780–788 (2009).
61. Minokawa, T., Rast, J. P., Arenas-Mena, C., Franco, C. B. & Davidson, E. H. Expression patterns of four different regulatory genes that function during sea urchin development. *Gene Expr. Patterns* **4**, 449–456 (2004).
62. Hejnol, A. *et al.* Assessing the root of bilaterian animals with scalable phylogenomic methods. *Proc. R. Soc. Lond. B Biol. Sci.* **276**, 4261–4270 (2009).

Acknowledgements

We are very grateful to Harriet Stephenson for help with the sea urchin RNA *in situ* hybridization. We acknowledge the Baylor College of Medicine Human Genome Sequencing Center, The Genome Institute at Washington University and the Broad Institute Genome Sequencing Platform for providing prepublication access to genome assemblies. We thank Sophie Martin, Hugh Robertson, Marcus Stensmyr and members of the Benton lab for discussions and comments on the manuscript. P.O.'s laboratory is supported by University College London and a Human Frontier Science Program Young Investigator Grant. F.R.'s laboratory is supported by the Sars Centre. Research in R.B.'s laboratory is supported by the University of Lausanne, European Research Council Starting Independent Researcher and Consolidator Grants (205202 and 615094) and the Swiss National Science Foundation (31003A_140869).

Author contributions

M.S. conceived the project, performed bioinformatics analyses and qPCR, morpholino injections and *in situ* hybridizations in *N. vectensis*, analysed data and wrote the manuscript. H.B. performed gene cloning, morpholino injections and *in situ* hybridizations in *N. vectensis*. C.S. performed morpholino injections and *in situ* hybridizations in *N. vectensis*. L.P. performed qPCR and *in situ* hybridizations in *S. purpuratus*. P.O. designed and performed qPCR and *in situ* hybridizations in *S. purpuratus*, analysed data and contributed to writing the manuscript. F.R. performed morpholino injections and *in situ* hybridizations in *N. vectensis*, analysed data and contributed to writing the manuscript. R.B. conceived and supervised the project, analysed data and wrote the manuscript.

Additional information

Supplementary Information accompanies this paper at <http://www.nature.com/naturecommunications>

Competing financial interests: The authors declare no competing financial interests.

Reprints and permission information is available online at <http://npg.nature.com/reprintsandpermissions/>

How to cite this article: Saina, M. *et al.* A cnidarian homologue of an insect gustatory receptor functions in developmental body patterning. *Nat. Commun.* 6:6243 doi: 10.1038/ncomms7243 (2015).